

# Laser Spectroscopy and Nuclear Structure

<http://www.physik.uni-mainz.de/Forschungsbericht/fb97/Image64.gif>

Study sizes and shapes of nuclei

- Isotope shifts
- Charge radii
- Nuclear moments ( $\mu$ ,  $Q$ )

Staple at ISOL facilities for many years

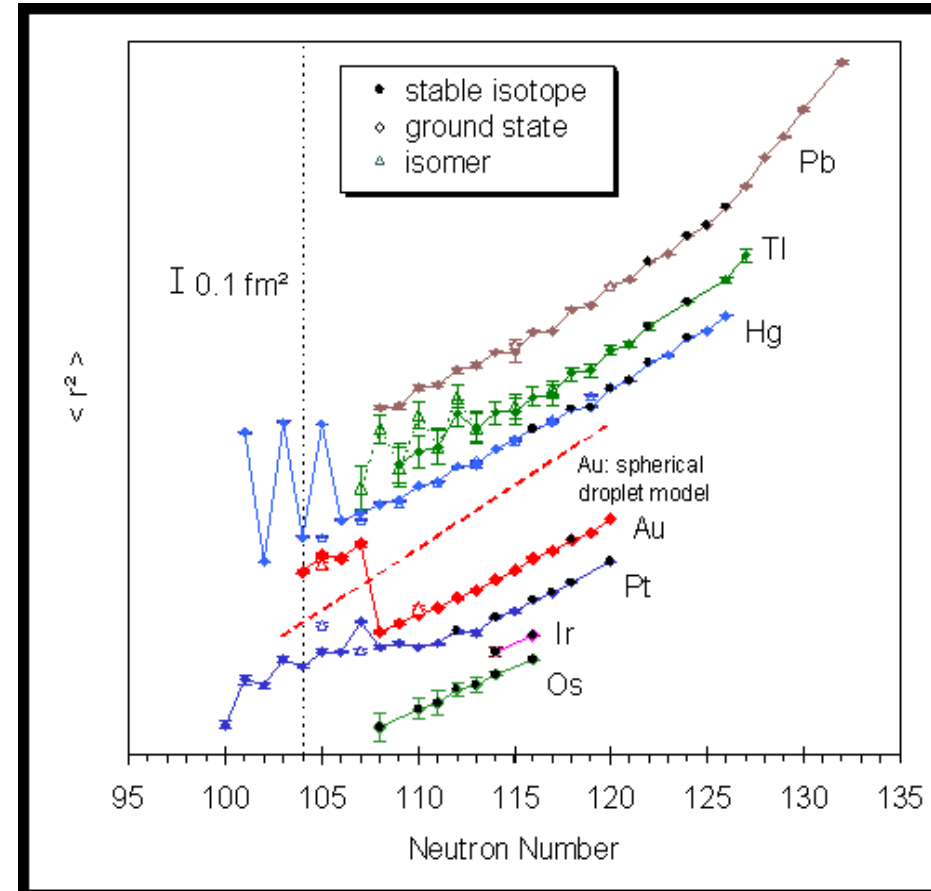
- CERN/ISOLDE
- JAEA
- Jyväskylä/IGISOL
- TRIUMF/ISAC

Extension to fast beam facilities

- BECOLA @ NSCL/MSU

Measurements made across long chains of isotopes

Method applicable to nuclides over wide range of  $T_{1/2}$  values



# Atomic Spectroscopy

**Spectroscopy** – absorption or emission of energy that induces transitions between states of a quantum mechanical system

**Atomic Spectroscopy** – transitions between electronic states in atom

The frequency at which energy is absorbed or emitted is related to the energy levels of the initial and final electronic states:

$$h\nu = |E_2 - E_1|$$

Electronic transitions typically have frequencies in the UV/Visible region of the electromagnetic spectrum

Selection rules govern the transitions that will be experimentally observed. The dipole approximation can be used to derive the selection rules for atomic spectroscopy (assuming L-S coupling applies)

$$\Delta\ell = \pm 1, \Delta L = 0, \pm 1, \Delta J = 0, \pm 1, \Delta S = 0$$

- $\Delta\ell$  is the angular momentum of the electron involved in the transition
- $\Delta L, \Delta J, \Delta S$  refer to the vector sums for all the electrons in the atom

# Quantum Numbers and Terms

many-electron atoms

Hydrogen atom has good quantum numbers  $n$ ,  $l$ ,  $m_l$ , and  $m_s$

These quantum numbers are not good for many-electron atoms or ions

no e-e repulsion	e-e repulsion and indistinguishable	spin-orbit	external magnetic field
Configuration	Terms	Levels	States
$n, l$	$L, S$	$J, M_J$	$J, M_J$

A useful model for atoms is to form vector sums of their orbital and spin angular momenta separately.

$L$ ,  $S$ ,  $M_L$  and  $M_S$  can then be considered good quantum numbers for many-electron atoms

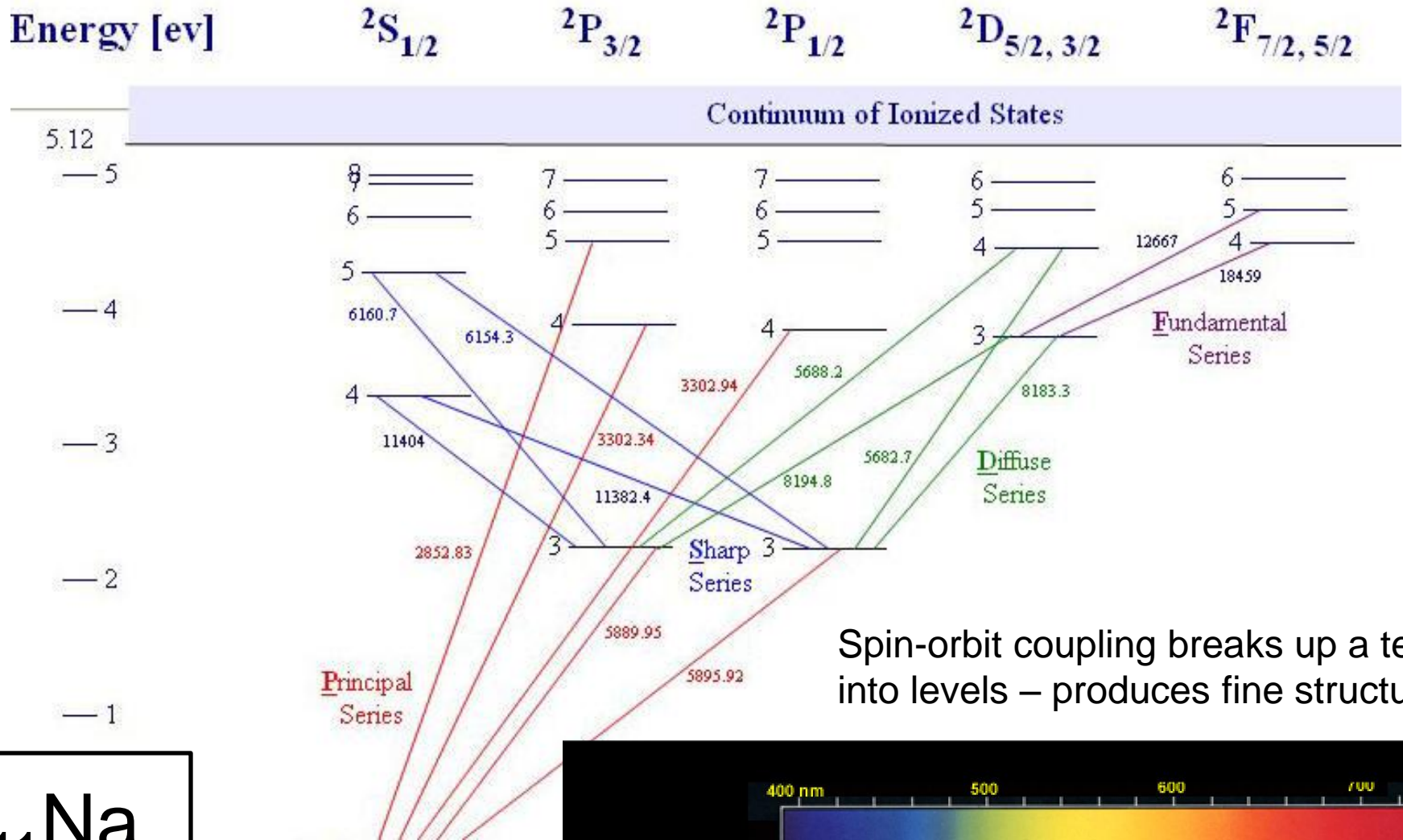
**Term** – group of states that has the same  $L$  and  $S$  values

Term Symbols  $(2S+1) L_J$

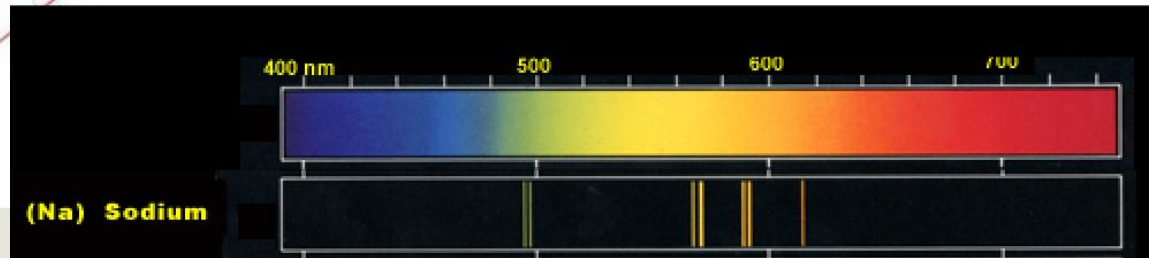
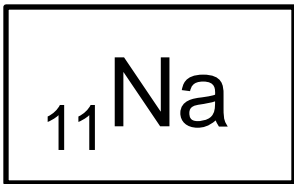
- $(2S+1)$  is the multiplicity
- $L=0, 1, 2, 3, \dots$  are given symbols S, P, D, F ...
- $J$  is the total angular momentum

$$J = L + S, L + S - 1, \dots, |L - S|$$

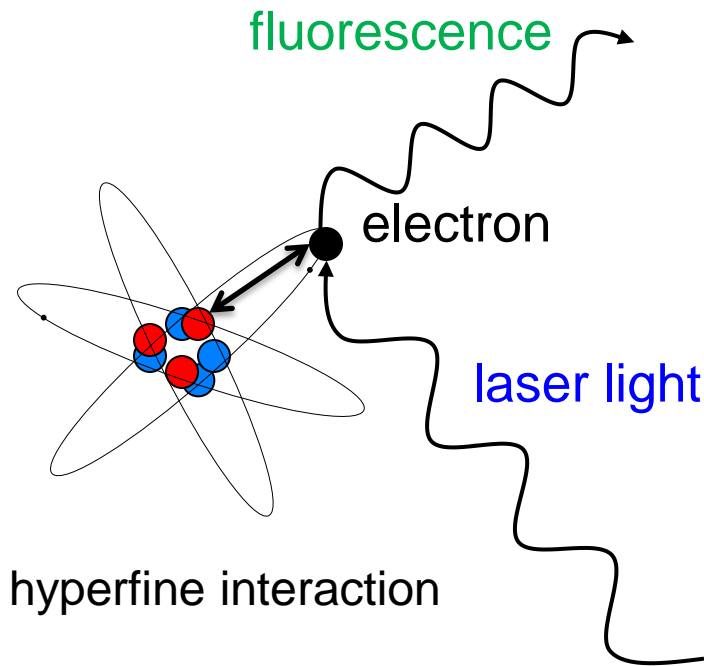
# Atomic Fine Structure



Spin-orbit coupling breaks up a term into levels – produces fine structure



# Atomic Hyperfine Structure



Interaction of atomic electron with the nucleus

Results in small shifts and splitting in the energy levels of atoms

Two main components of interaction:

Magnetic Dipole and Electric Quadrupole

Electric Dipole Component:

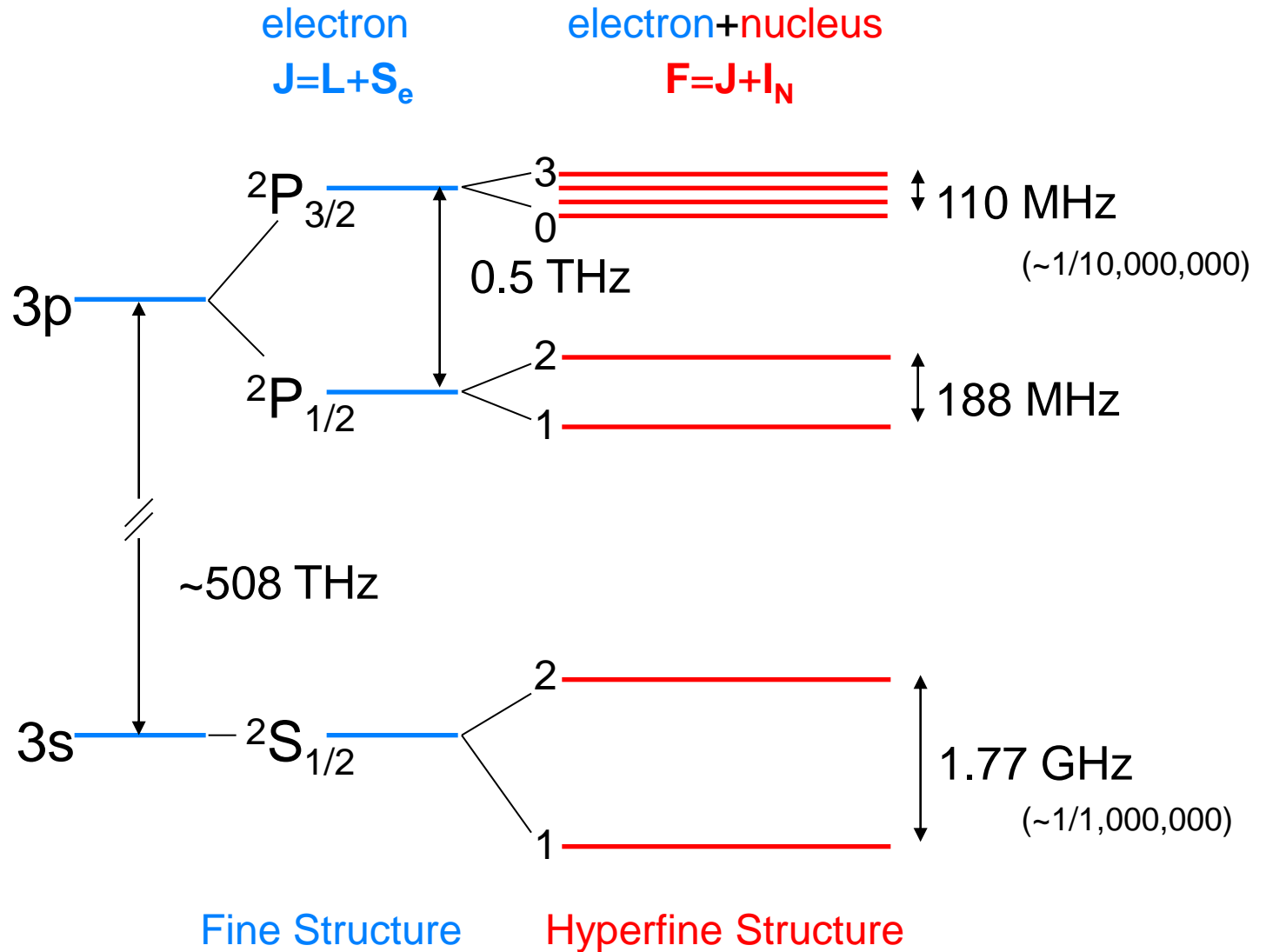
Interaction of magnetic dipole moment of the nucleus ( $I > 0$ ) with the magnetic field experienced by the nucleus associated with the orbital and spin angular momentum of the electrons

Electric Quadrupole Component:

Interaction of the electric quadrupole moment of the nucleus ( $I \geq 1$ ) with the electric field gradient due to the distribution of charge within the atom

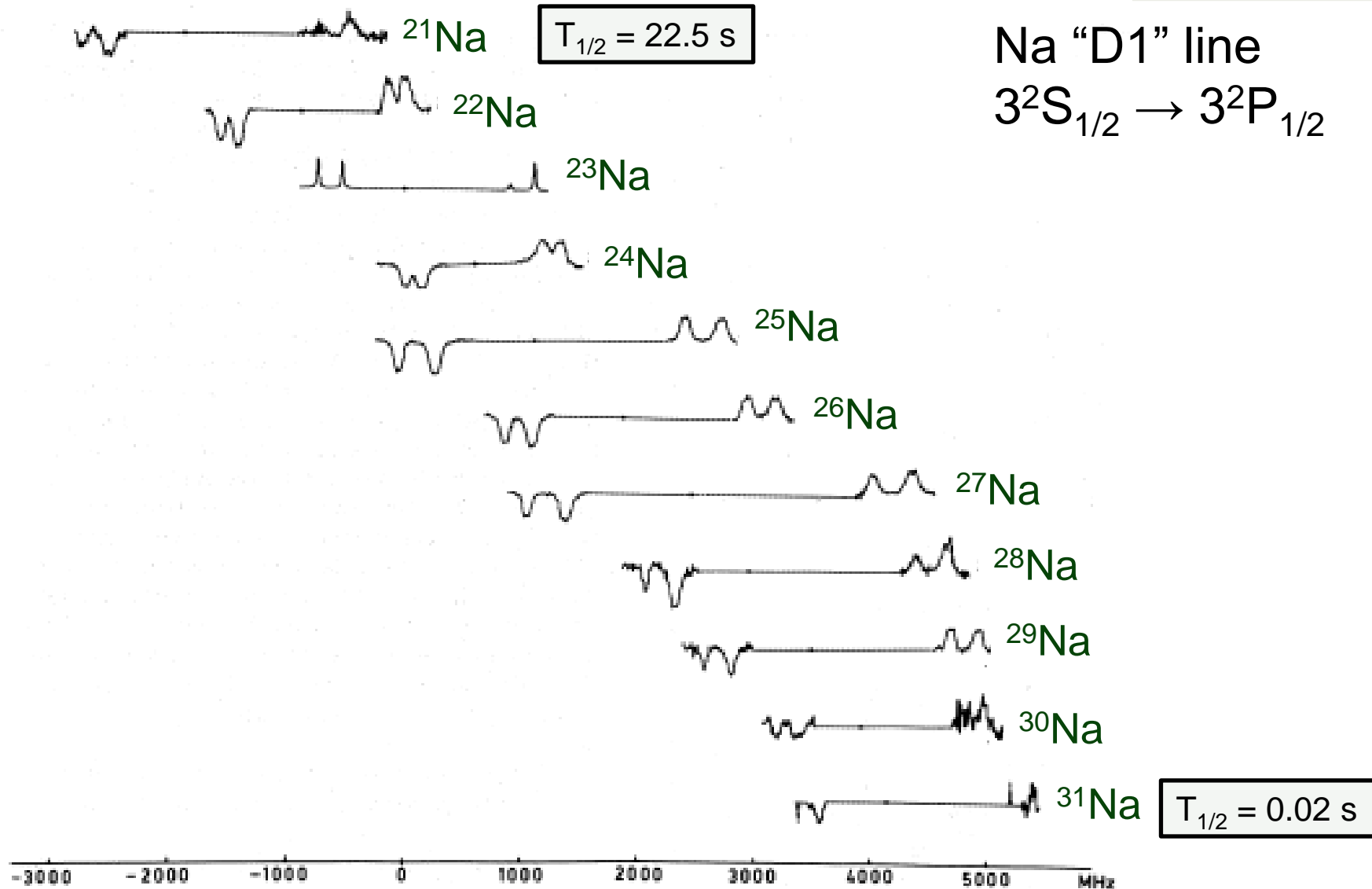
# Atomic Hyperfine Structure

$^{23}\text{Na}$  ( $I_N=3/2$ )



$$F = J + I_N, J + I_N - 1, \dots, |J - I_N|$$

# Sodium Laser Hyperfine Spectra



# Hyperfine Energy Shift

The hyperfine energy shift can be derived from the Hamiltonian the describes the hyperfine structure for each transition component

$$\Delta E_{hfs} = \frac{1}{2} A_{hfs} K + B_{hfs} \frac{\frac{3}{2} K(K+1) - 2I_N(I_N+1)J(J+1)}{2I_N(2I_N-1)2J(2J-1)}$$

where

$$K = F(F+1) - I_N(I_N+1) - J(J+1)$$

$A_{hfs}$  is the magnetic dipole constant and is proportional to  $\mu B_e$

$B_{hfs}$  is the electric quadrupole constant and is proportional to  $eqQ$



# Hyperfine Structure Constants: $^{23}\text{Na}$

Magnetic Dipole Constant, $3^2\text{S}_{1/2}$	$A_{\text{hfs}}(3^2\text{S}_{1/2})$	885.813 MHz
Magnetic Dipole Constant, $3^2\text{P}_{1/2}$	$A_{\text{hfs}}(3^2\text{P}_{1/2})$	94.44 MHz
Magnetic Dipole Constant, $3^2\text{P}_{3/2}$	$A_{\text{hfs}}(3^2\text{P}_{3/2})$	18.534 MHz
Electric Quadrupole Constant, $3^2\text{P}_{3/2}$	$B_{\text{hfs}}(3^2\text{P}_{3/2})$	2.724 MHz

Average magnetic field at nucleus from atomic electrons

$$A_{\text{hfs}} = \frac{\mu_I \langle H_e(0) \rangle}{IJ}$$

Average gradient of the electric field generated by the electrons at the nucleus

$$B_{\text{hfs}} = eQ \langle V_{zz}(0) \rangle$$

$$\mu_I(^{23}\text{Na}) = +2.217 \mu_N$$

$$Q(^{23}\text{Na}) = +0.109 \text{ b}$$

# Reference Measurements

The nuclear moments are usually deduced relative to a well-known reference measurement

- Eliminates the need to explicitly know  $\langle H_e(0) \rangle$  and  $\langle V_{zz}(0) \rangle$
- High precision reference measurements are available for stable isotopes

$$A_{hfs} = \frac{\mu_I \langle H_e(0) \rangle}{IJ}$$

$\Delta$  is the hyperfine anomaly, and represents the distribution of magnetization across the nuclear volume (the Bohr-Weisskopf effect)

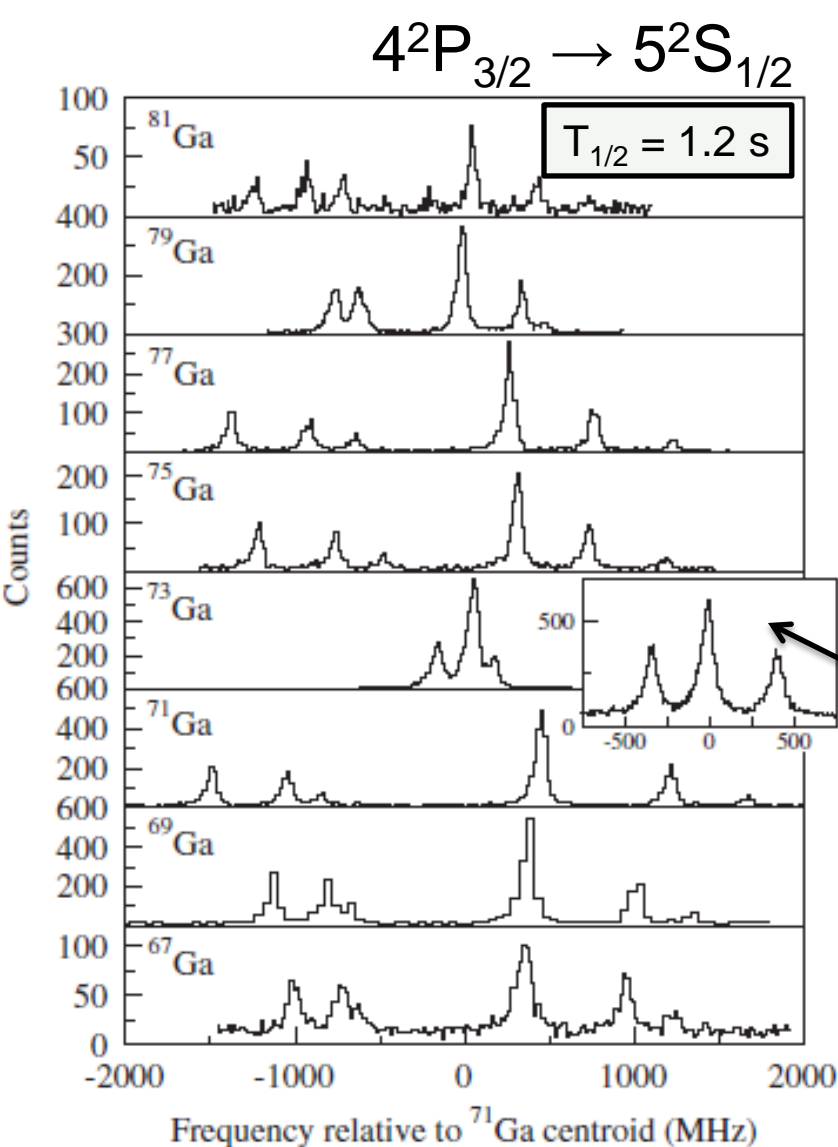
$$\mu_I = \mu_{ref} \frac{A}{A_{ref}} \frac{I}{I_{ref}}$$

For light nuclei, it is sufficient to treat the nuclear as a point with a pure dipole field.

$$\mu_I = (1 + \Delta) \mu_{ref} \frac{A}{A_{ref}} \frac{I}{I_{ref}}$$

In heavy nuclei, the  $S_{1/2}$  and  $P_{1/2}$  state wavefunctions both significantly overlap the nucleus, leading to a large value of  $\Delta$

# Hyperfine Spectra of the Ga isotopes



Hyperfine spectra reveal very different structure for  $^{73}\text{Ga}$  compared to other odd-A isotopes

The number of peaks and relative intensities of the transitions will depend on the nuclear spin ( $I_N$ )

<i>A</i>	<i>I</i>	$A(^2S_{1/2})$ (MHz)	$A(^2P_{3/2})$ (MHz)	$B(^2P_{3/2})$ (MHz)
67	3/2	+979.7(2.5)	+175.8(1.0)	+73(4)
69	3/2	+1069.5(1.5)	+191.5(9)	+63(2)
71	3/2	+1358.2(1.6)	+242.8(7)	+39(2)
73	1/2	+332(3)	+60.7(1.3)	0
75	3/2	+973.1(1.5)	+173.6(9)	-104.9(1.3)
77	3/2	+1070.6(1.2)	+191.8(5)	-76.7(1.5)
79	3/2	+555.0(1.4)	+98.3(9)	+58.2(1.5)
79	5/2	+369.5(0.6)	+64.5(4)	+118.6(2.1)
81	3/2	+831.2(1.6)	+138.4(8)	-43.4(1.8)
81	5/2	+555.6(1.3)	+98.9(4)	-17.7(2.7)

# Isotope Shifts

**Isotope Shift** – change in characteristic spectral line due to change in isotope

$$\delta\nu^{A,A'} = \nu^{A'} - \nu^A = \delta\nu_{MS} + \delta\nu_{FS}$$

where  $\nu$  is the center of gravity of the hyperfine components for each isotope

**Mass Shift** ( $\delta\nu_{MS}$ ) – accounts for the difference in the relative motion between the nucleus (with mass number  $A$ ) and electron

Change in reduced mass (easy)

$$\delta\nu_{MS} = k \frac{m_{A'} - m_A}{m_{A'} m_A}$$

$$k = k_{NMS} + k_{SMS}$$

Electron correlations (difficult)

**Field Shift** ( $\delta\nu_{FS}$ ) – proportional to the finite size of the nuclear charge distribution

$$\delta\nu_{FS} = F_e \delta \langle r^2 \rangle^{A,A'}$$

Electronic Part                      Nuclear Part

$$F_e = -\frac{Ze^2}{6\epsilon_0} \Delta |\varphi(0)|^2$$

Change in electron density at nucleus between spectroscopic states

# Mass and Field Shifts

The Mass Shift ( $\delta v_{MS}$ ) dominates the Isotope Shift of low-Z elements, as the relative mass difference is large for any two isotopes.

$$\text{light nuclei: } \delta v_{MS} \sim 10^4 \times \delta v_{FS}$$

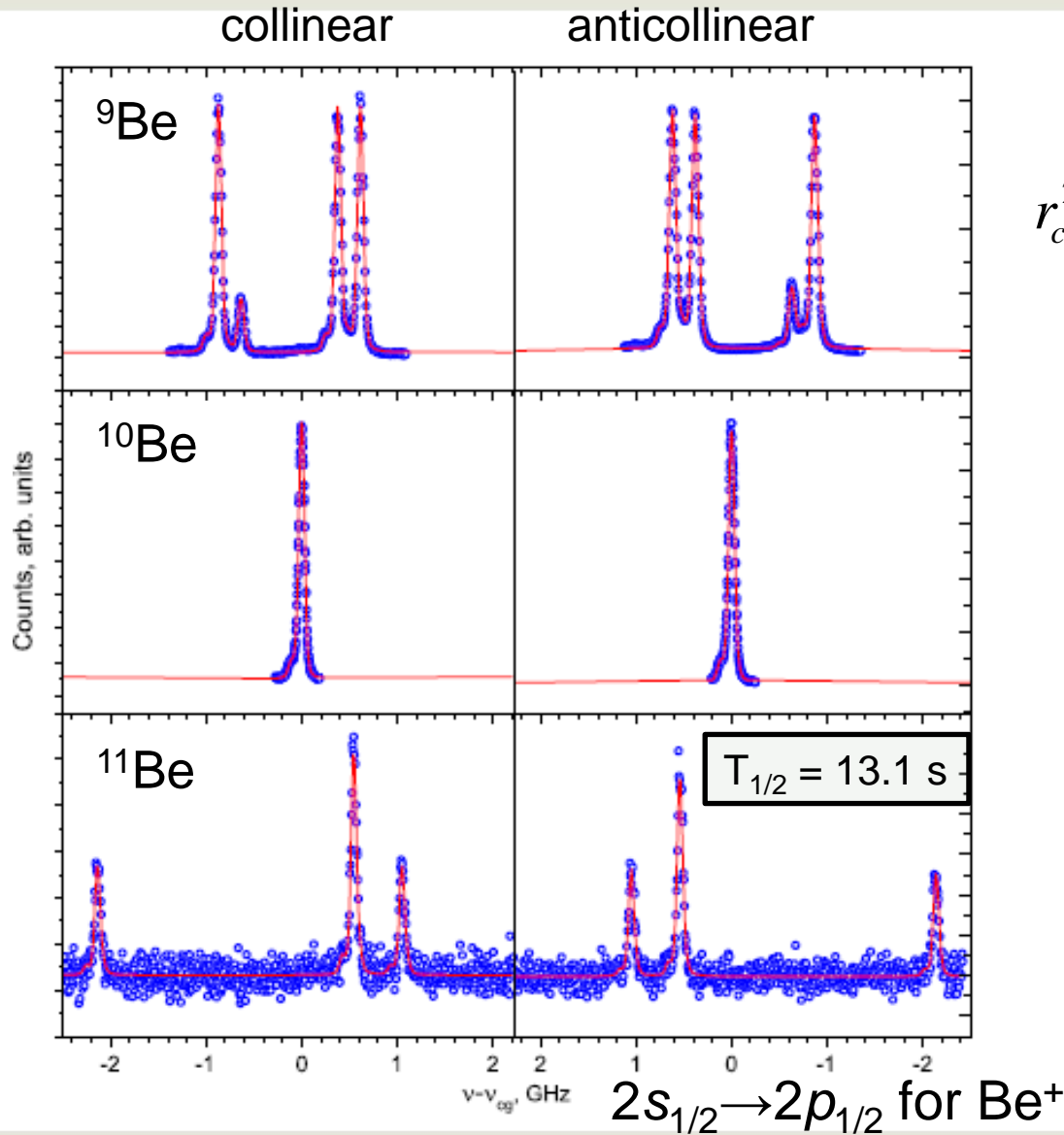
However, it is the Field Shift ( $\delta v_{FS}$ ) that provides the desired nuclear information

$$\delta v_{FS} \propto \delta \langle r^2 \rangle^{A,A'}$$

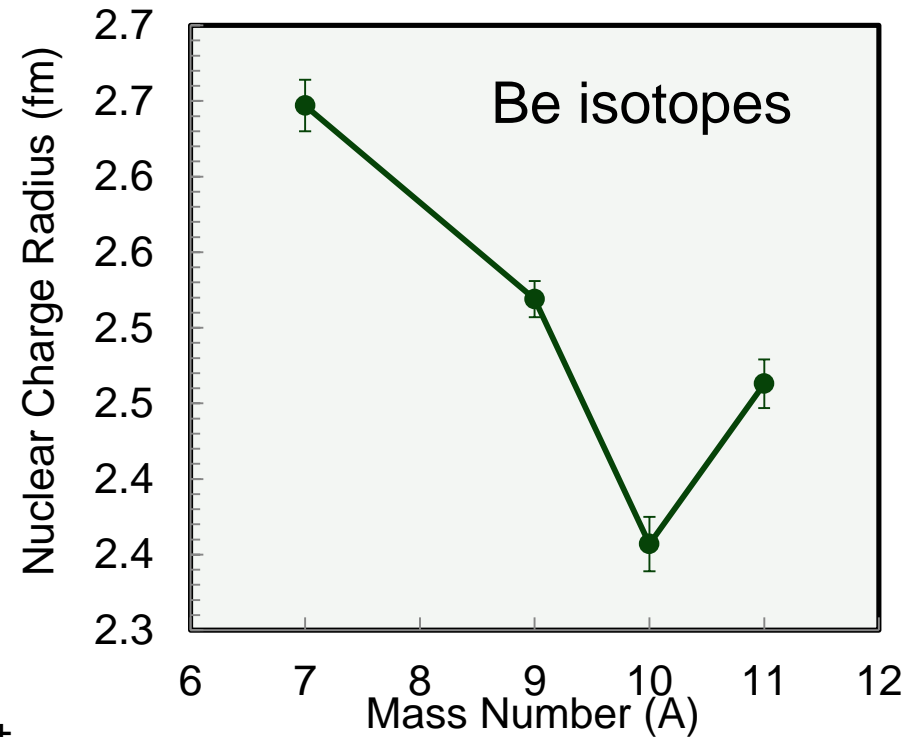
**Charge radius** ( $\langle r^2 \rangle$ ) – The root-mean-square (rms) charge radius is a measure of the size of an atomic nucleus, and can be measured by both electron scattering and atomic spectroscopy.

Optical measurements only provide the change in  $\langle r^2 \rangle$  between two isotopes; therefore, determination of the absolute charge radius ( $r_c$ ) requires reference to a (well) known value in the isotopic chain.

# Charge Radius of Be isotopes



$$r_c^2({}^A\text{Be}) = r_c^2({}^9\text{Be}) + \frac{\overset{\text{theory}}{\delta v_{IS}^{9,A}} - \overset{\text{measurement}}{\delta v_{MS}^{9,A}}}{-16.912 \text{ MHz/fm}^2}$$



# Laser Spectroscopy Methods

## Collinear Laser Spectroscopy

- Fluorescence photon detection
  - » Na, Ga, and Be already presented
- Beta-detected nuclear magnetic resonance
  - » Neutron-rich  $^{31,33}\text{Mg}$  isotopes
  - » Production rate  $10^3$  ions/s for  $^{33}\text{Mg}$
- Collisional ionization and ion counting
  - » Neutron-rich Ar isotopes
  - » Production rate  $\sim 10^6$  ions/s for  $^{43}\text{Ar}$

## Resonance Ionization Spectroscopy

- Ion counting
  - » Neutron-rich Sn isotopes
  - » Production rate  $\sim 10^8$  ions/s for  $^{132}\text{Sn}$

## In-Source Laser Spectroscopy

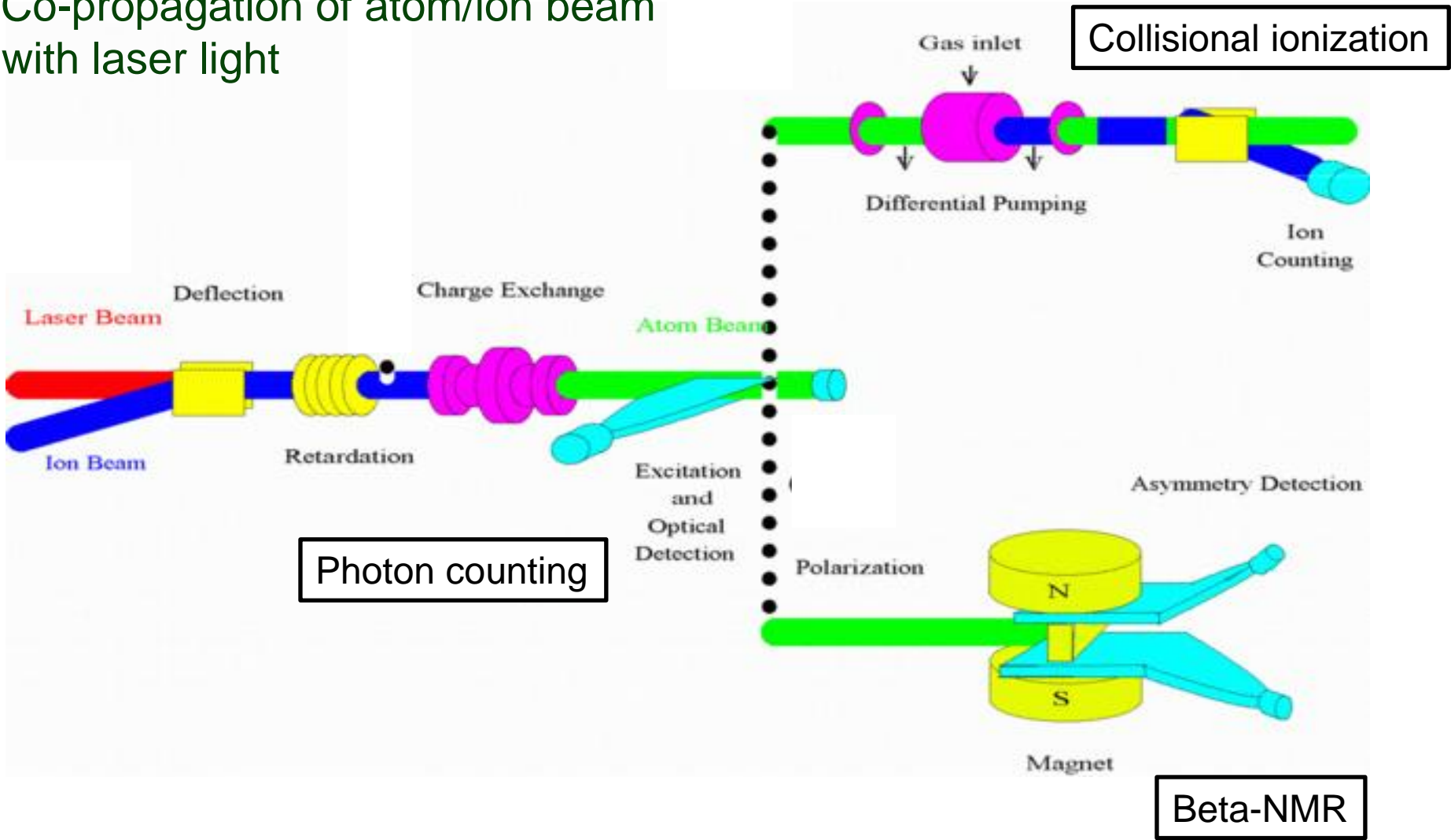
- Ion Counting
  - » Neutron-deficient Cu isotopes
  - » Production rate 6 ions/s for  $^{57}\text{Cu}$

## Spectroscopy in Traps

- Fluorescence photon detection
  - »  $^{6,8}\text{He}$  isotopes
  - » Production rate  $10^5$  ions/s for  $^8\text{He}$

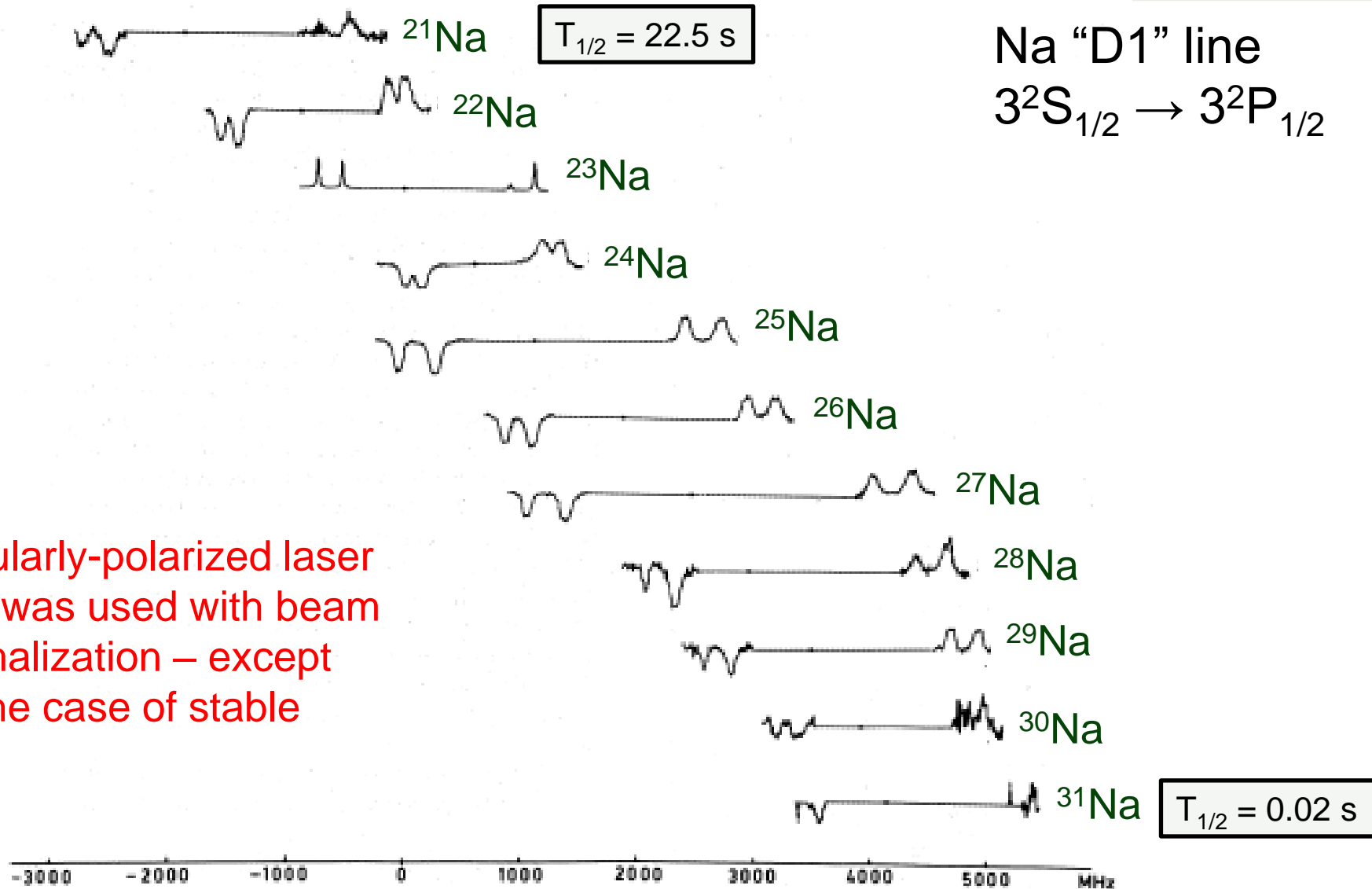
# Collinear Laser Spectroscopy

Co-propagation of atom/ion beam with laser light



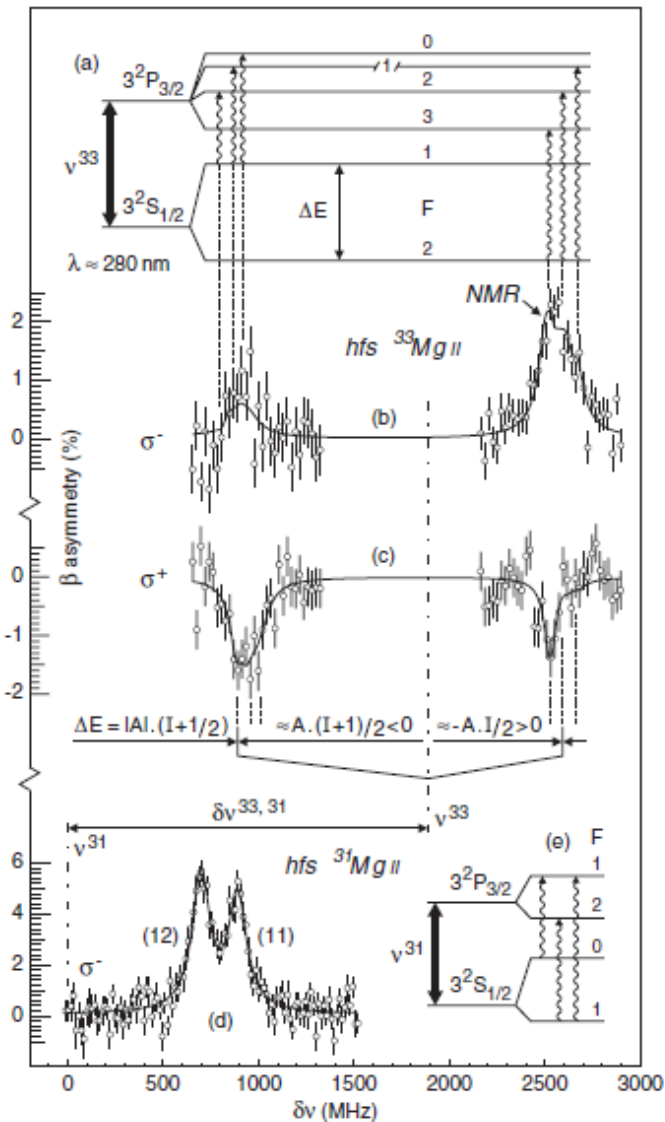
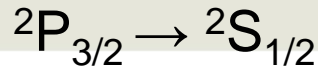


# Revisit: Sodium Laser Hyperfine Spectra



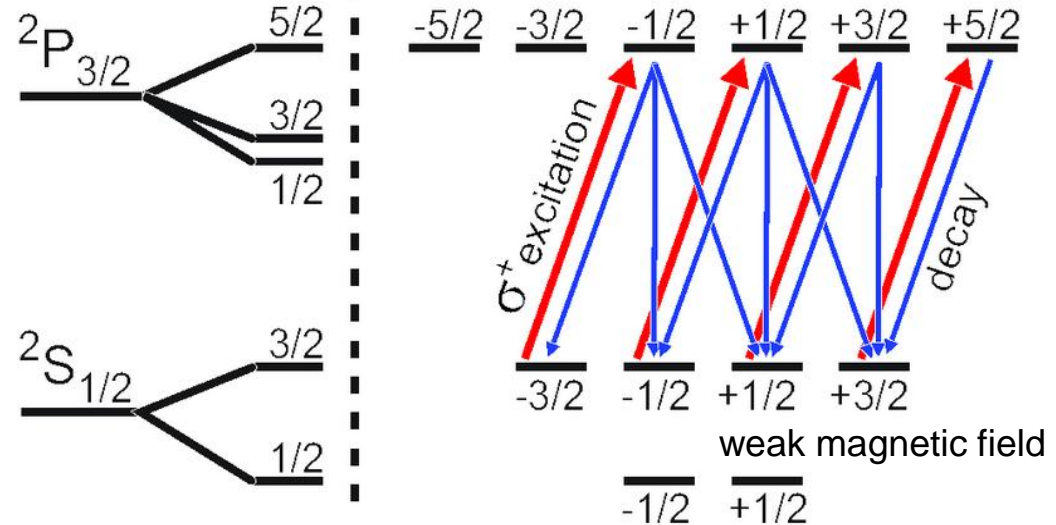
Circularly-polarized laser light was used with beam normalization – except for the case of stable  $^{23}\text{Na}$

# Optical Pumping and Hyperfine Structure



Atom/ion beam is overlapped with laser light that is circularly polarized

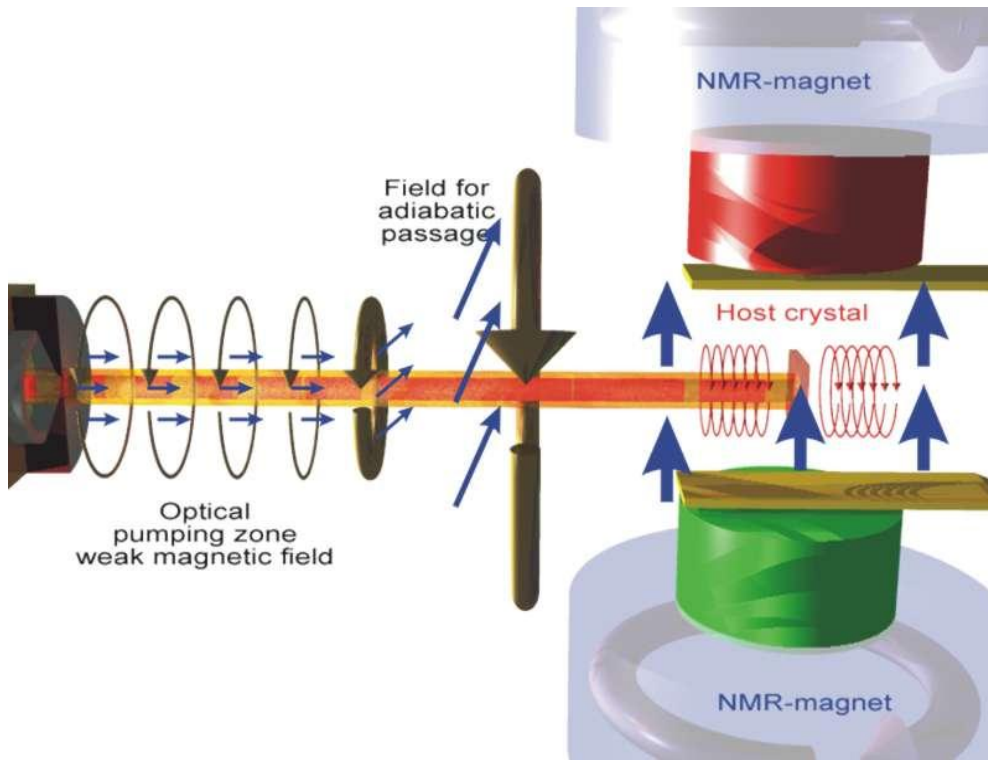
$D_2$  line in  $\text{Mg}^+$



Spin polarized beam implanted in a host crystal at the center of a dipole magnet

Beta-counting asymmetry measured as a function of laser frequency

# Beta-detected Nuclear Magnetic Resonance

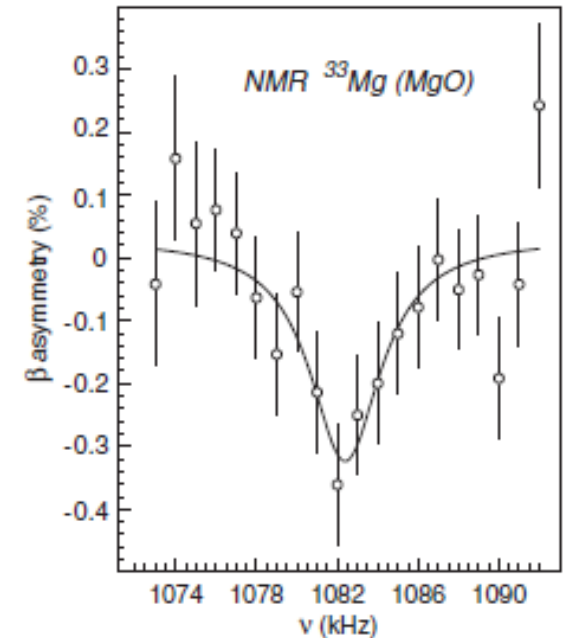


Atom/ion beam is polarized by optical pumping

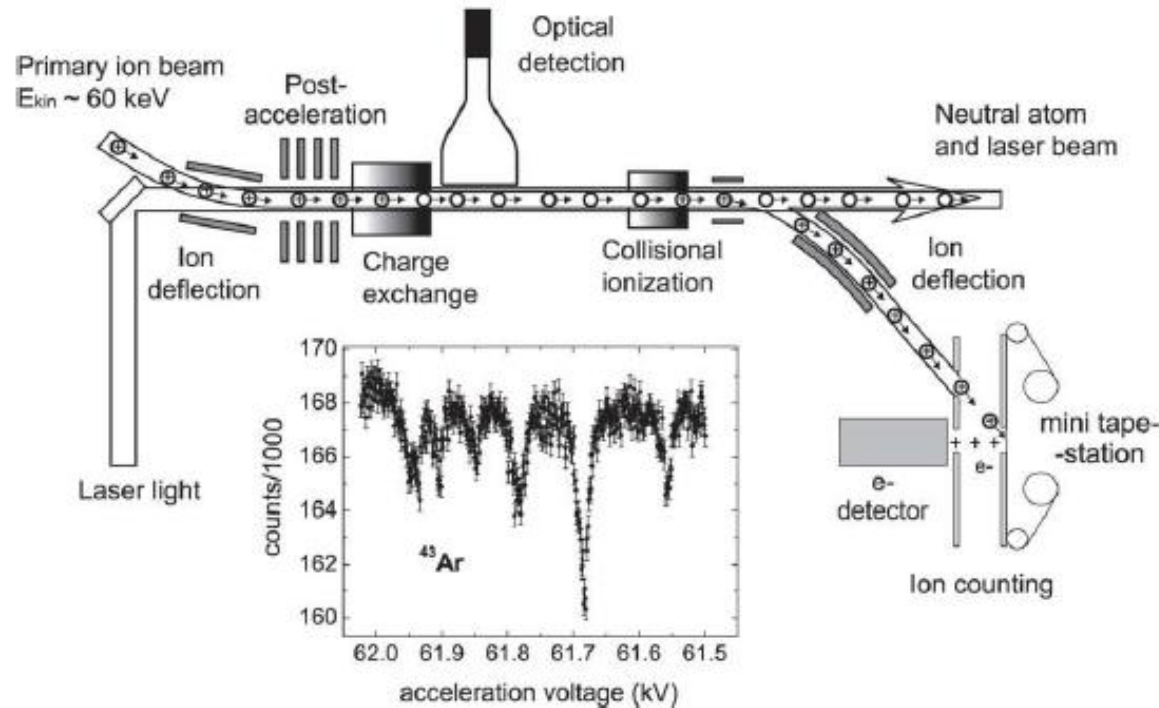
Atomic spin is rotated adiabatically in the NMR fringe field. Nuclear and electron spins decouple in strong NMR field.

Spin polarized beam implanted in a host crystal at the center of a dipole magnet

Beta-counting asymmetry measured as a function of applied radiofrequency



# State Selective Collisional Ionization



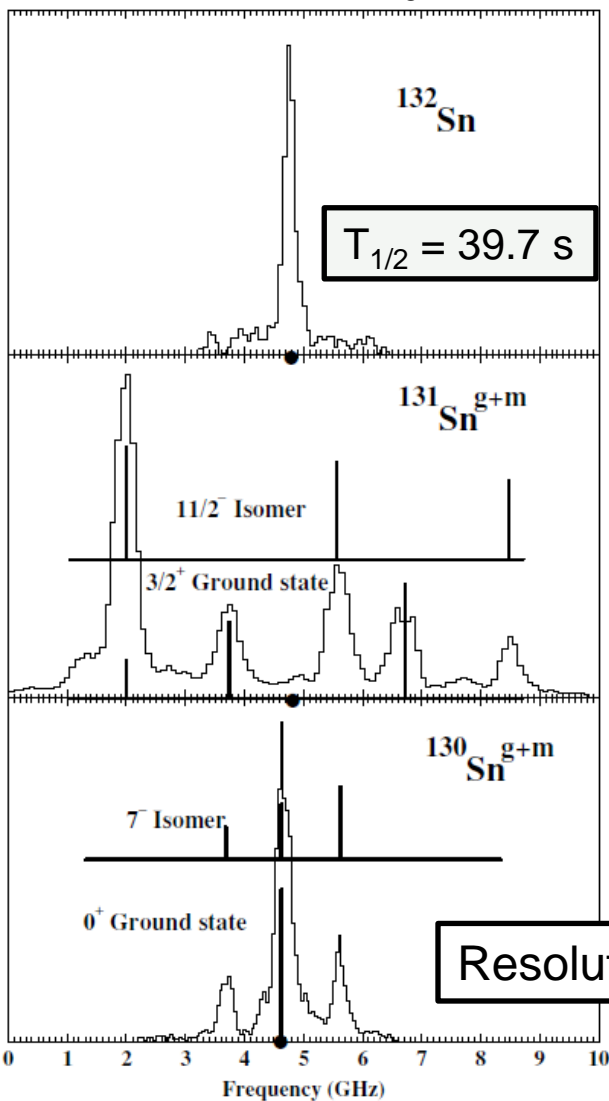
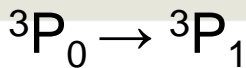
Ar isotopes produced by spallation at CERN/ISOLDE

Laser light was co-propagated with  $\text{Ar}^+$  ions, metastable state in Ar atom populated by near-resonant charge exchange with K vapor

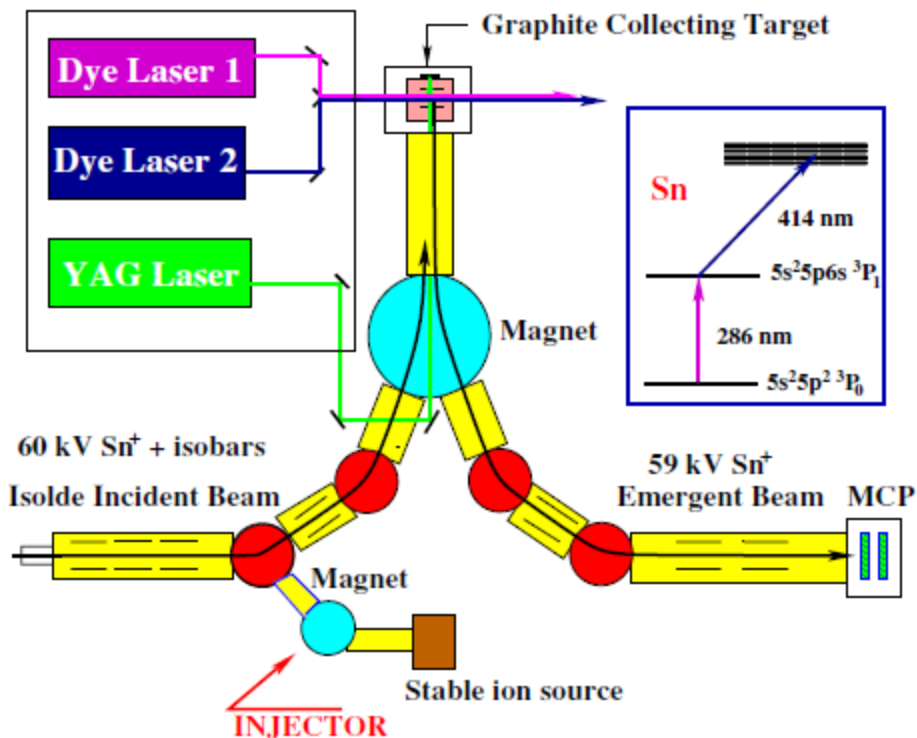
Atoms selectively re-ionized in  $\text{Cl}_2$  gas. Again, metastable state is favored

Spectroscopy was performed by measuring the ion current as a function of the frequency of a pump laser driving the atoms from the metastable state to the ground  $^1S_0$  state

# Resonance Ionization Spectroscopy



Sn isotopes deposited into C collector and laser desorbed to produce atomized sample  
 Laser light was used to resonantly-ionize the atoms  
 Spectroscopy was performed by measuring the ion current as a function of laser frequency

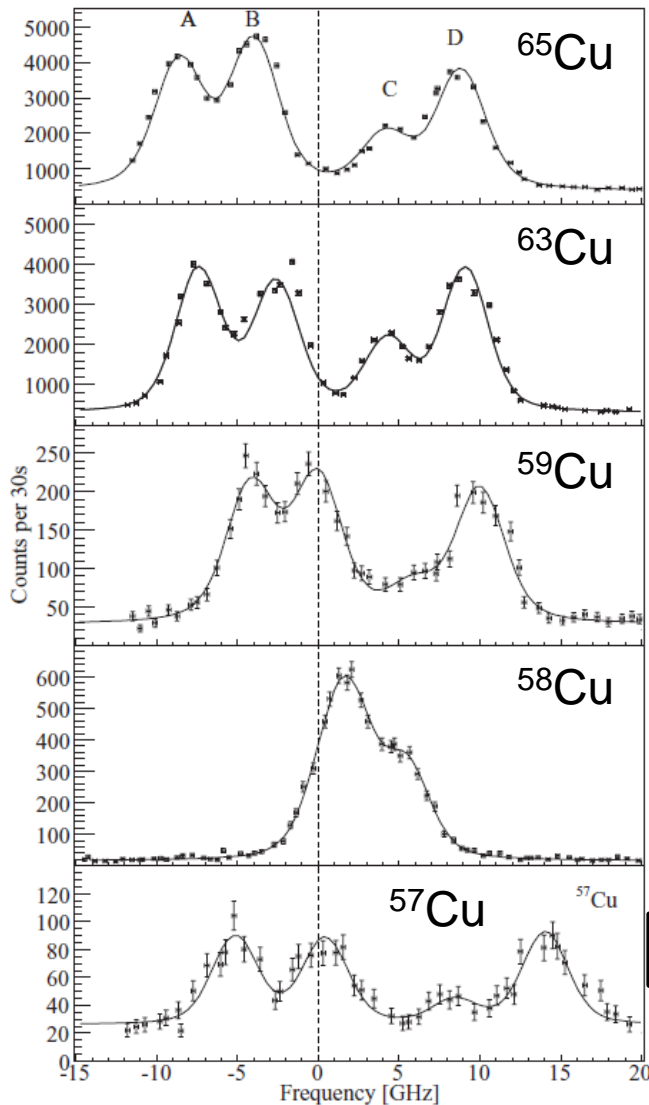
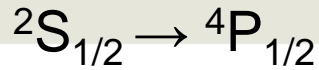


LeBlanc et al., PRC 72, 034305 (2005)

Krönert et al., NIM A300, 522 (1991)

Mantica, EBSS 2011, Slide 21

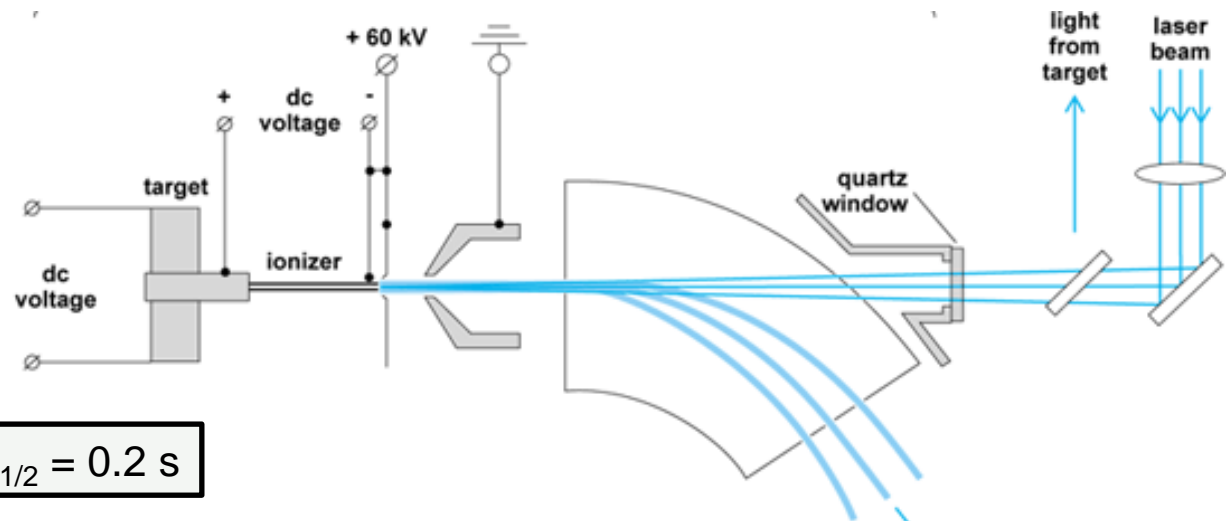
# In-Source Spectroscopy



Cu isotopes produced at Leuven Isotope Separator On-Line facility using fusion evaporation reactions

Recoils were transported by gas flow to an ionization chamber, and laser light was used to produce  $\text{Cu}^+$

Spectroscopy was performed by scanning the laser frequency of the first step of the ionization process



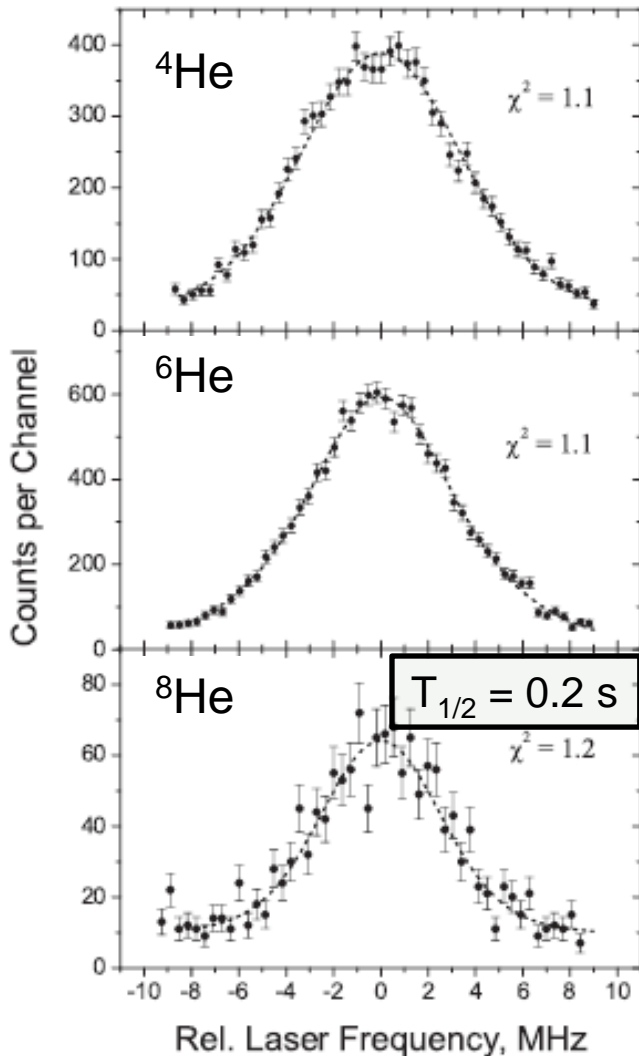
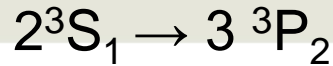
Gas cell pressure was the main source of line broadening

Cocolios et al., PRL 103, 102501 (2009)

Seliverstov et al., HI 127, 425 (2000)

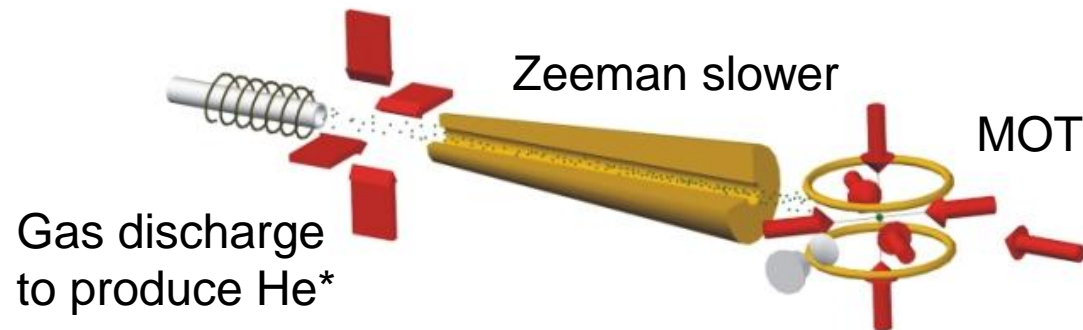
Mantica, EBSS 2011, Slide 22

# Spectroscopy in Traps



${}^6,{}^8\text{He}$  produced by fragmentation in a thick graphite target heated to  $\sim 2000$  K

Recoils were transported to a graphite foil for neutralization. Neutralized He atoms were then pumped into the atomic beam apparatus

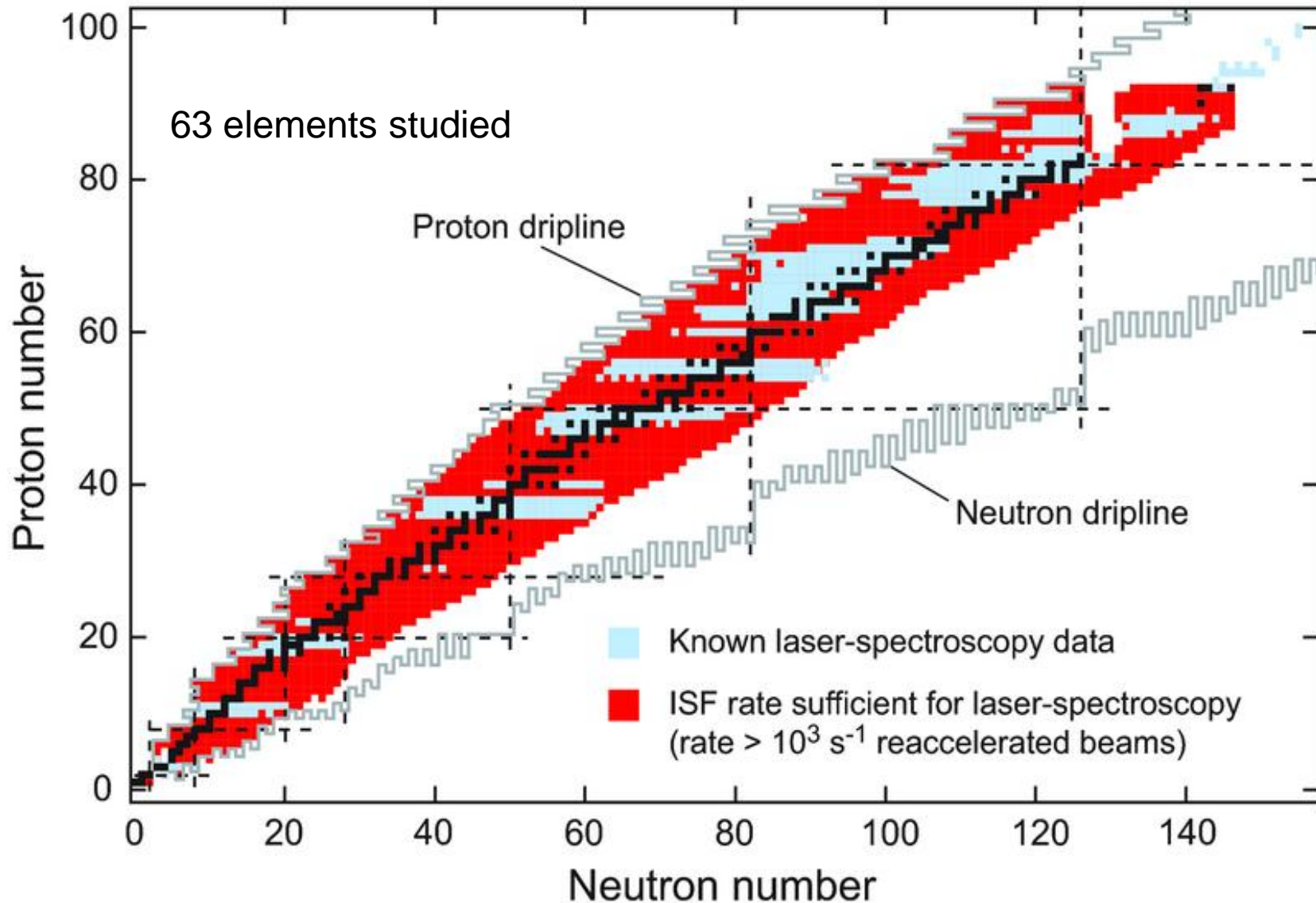


Magneto-optic trap (MOT) was used to capture the metastable He ions. The trapping laser was set to the cycling  $2^3S_1 \rightarrow 2^3P_2$  transition at 1083 nm

Spectroscopy was performed by scanning the laser frequency of the  $2^3S_1 \rightarrow 3^3P_2$  transition and observing the fluorescence signal

# Elements Studied by Laser Spectroscopy

Adapted from Kluge and Nörterhäuser, Spectrochimica Acta B 58, 1031 (2003)





# Collinear Laser Spectroscopy: Principles

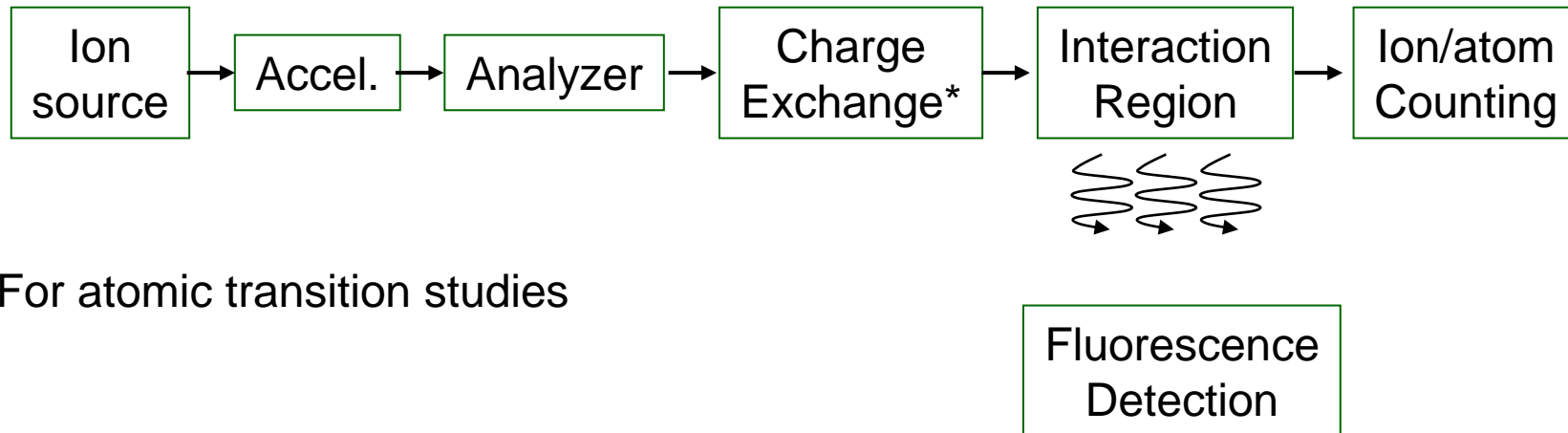
Superposition of ion/atom beam with propagating laser beam

Resonance achieved by either laser frequency tuning or beam velocity changes

Atomic studies require beam neutralization (with charge exchange cell)

Large photon absorption cross section

Laser linewidth much narrower than atomic linewidth



\* For atomic transition studies

Nearly Doppler-broadening free method (due to particle acceleration)

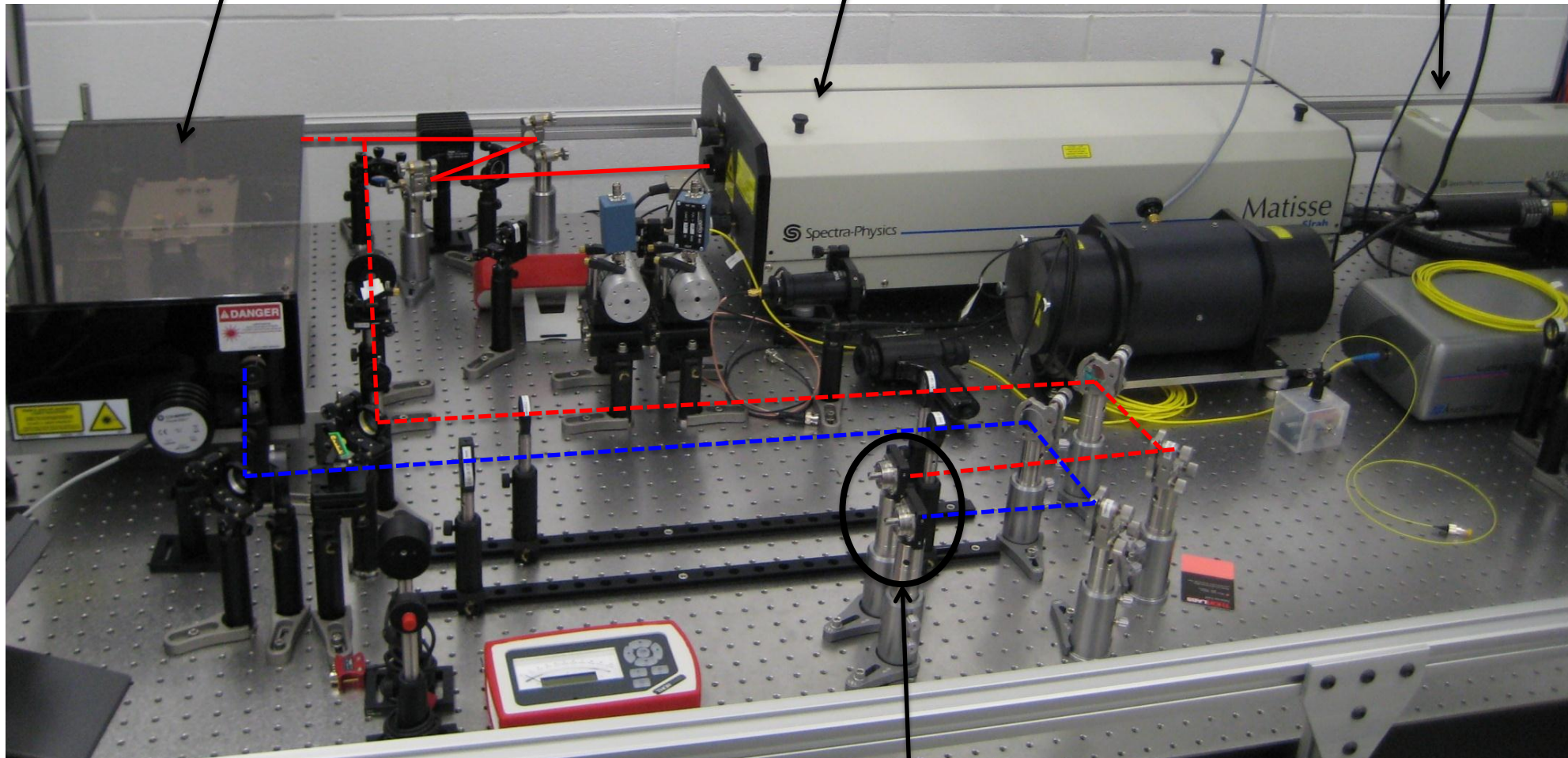
Applicable to ions or atoms

# NSCL Solid-State Laser System

Frequency Doubler  
350 - 500 nm

Ti:Saph  
700 - 1000 nm

Diode Pump Laser  
532 nm



Optical Coupling

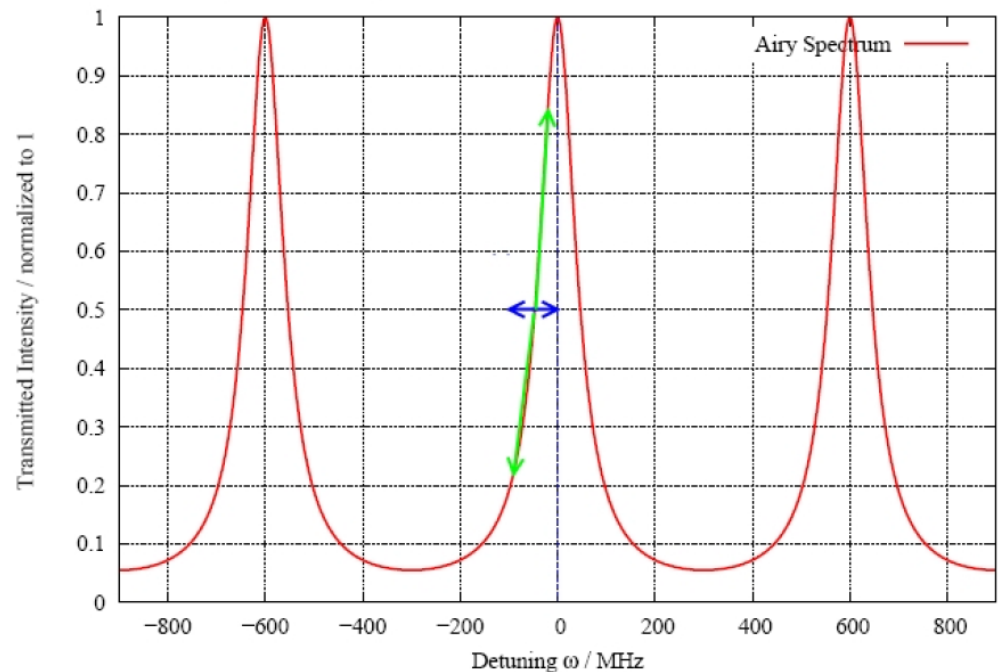
# Laser System Stabilization

- Short term stabilization (ms) is done with a resonator cavity that provides a feedback loop to a fast piezoelectric actuator to stabilize the system.
  - Stabilization of  $< 1$  MHz has been achieved.
- Long term stabilization (hr) is achieved via a He:Ne locking scheme.
  - The He:Ne atomic transition of 633 nm is used to lock the Ti:Sapphire laser.
  - Stabilization of  $< 8$  MHz has been achieved.
  - Note: The absolute frequency ( $10^{-7}$  precision) is not known.

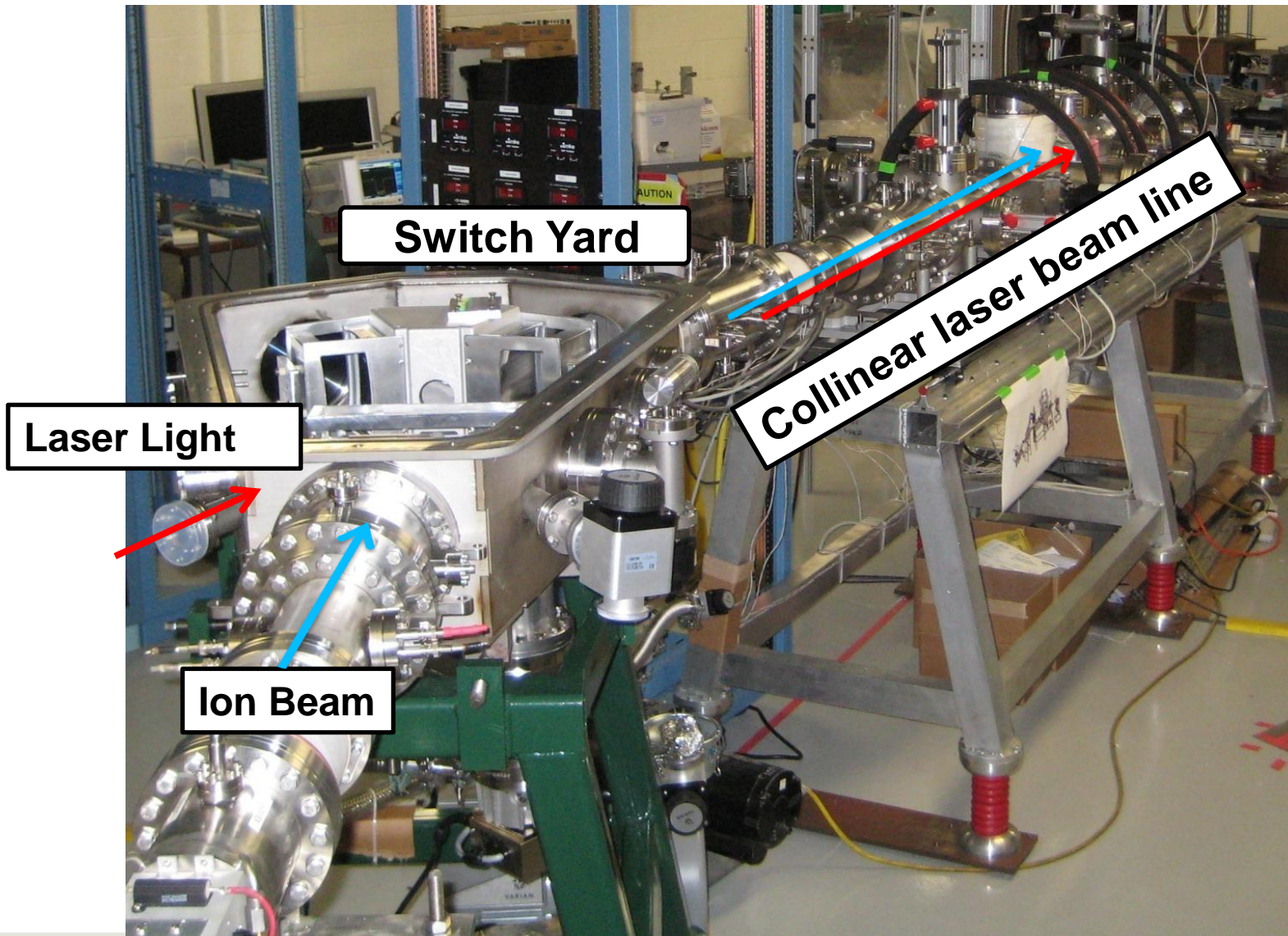
Solutions to the absolute frequency issue:

- Reference measurement
- Frequency comb

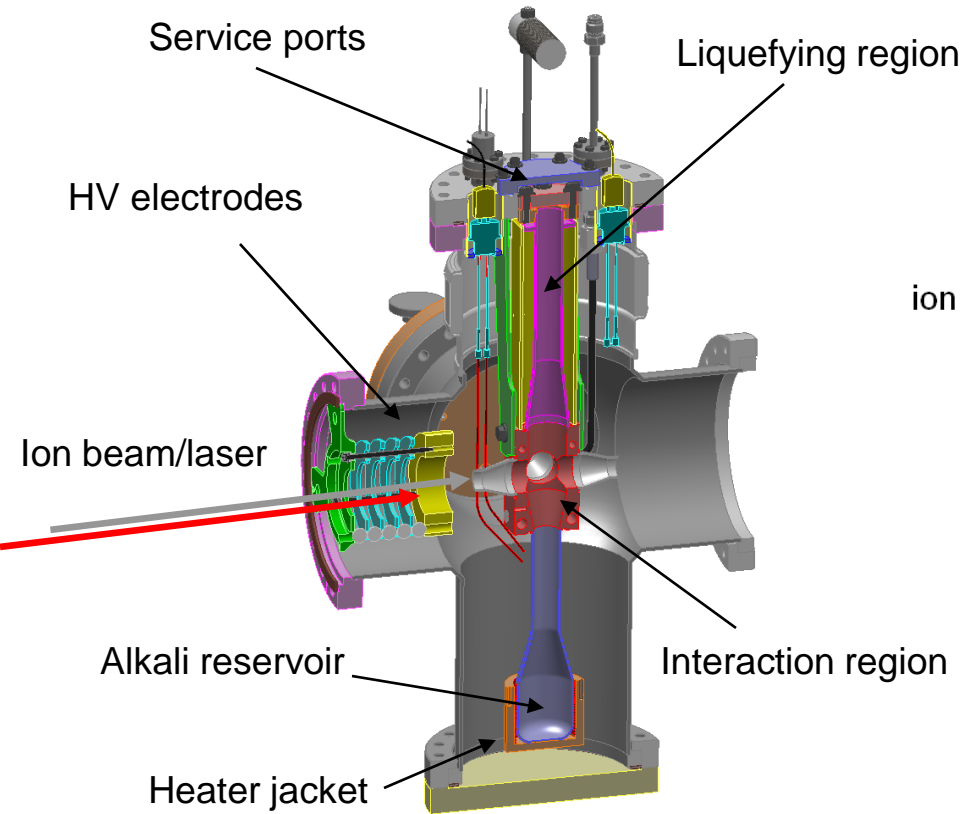
Airy Transmission signal for a resonator with FSR = 600 MHz and Finesse = 17.



# NSCL Laser Spectroscopy Beam Line

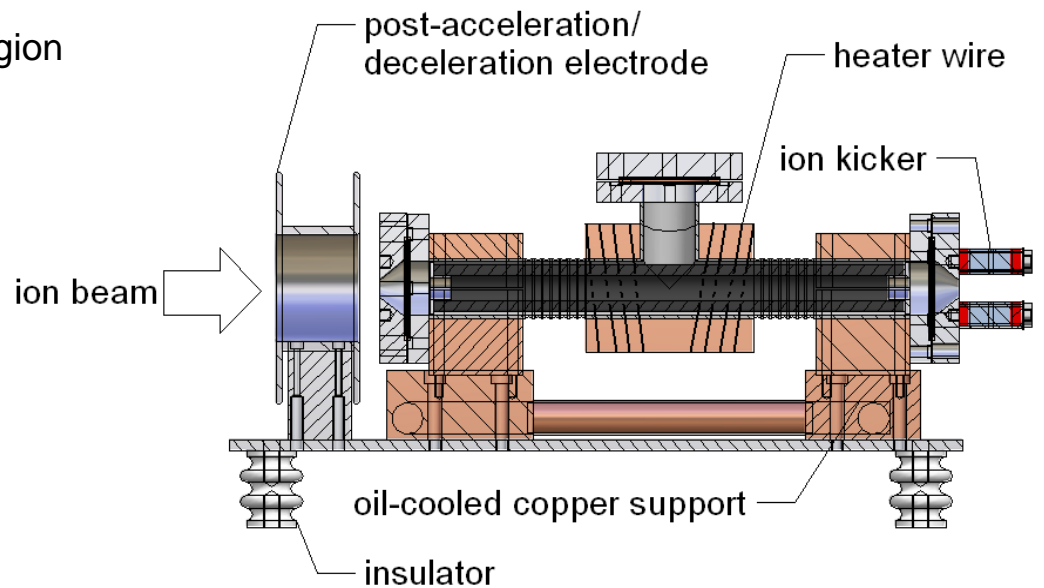


# Charge Exchange Cells

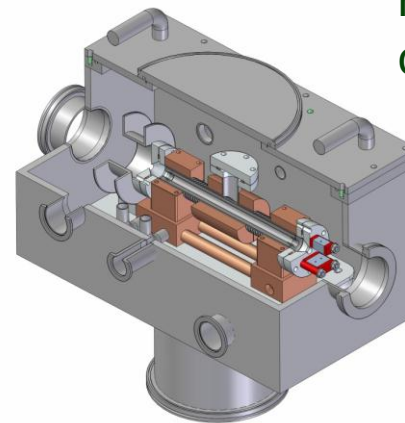


NSCL

vertical configuration  
cold end on one side



horizontal configuration  
cold end on both sides

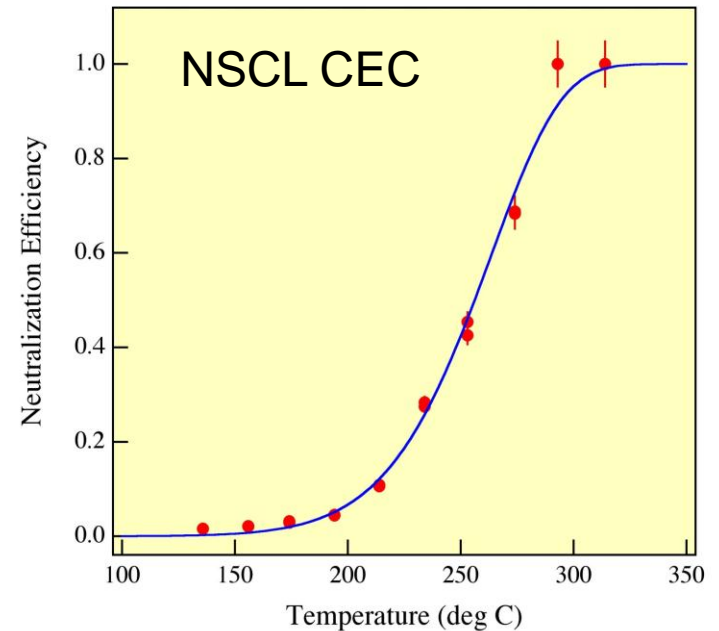
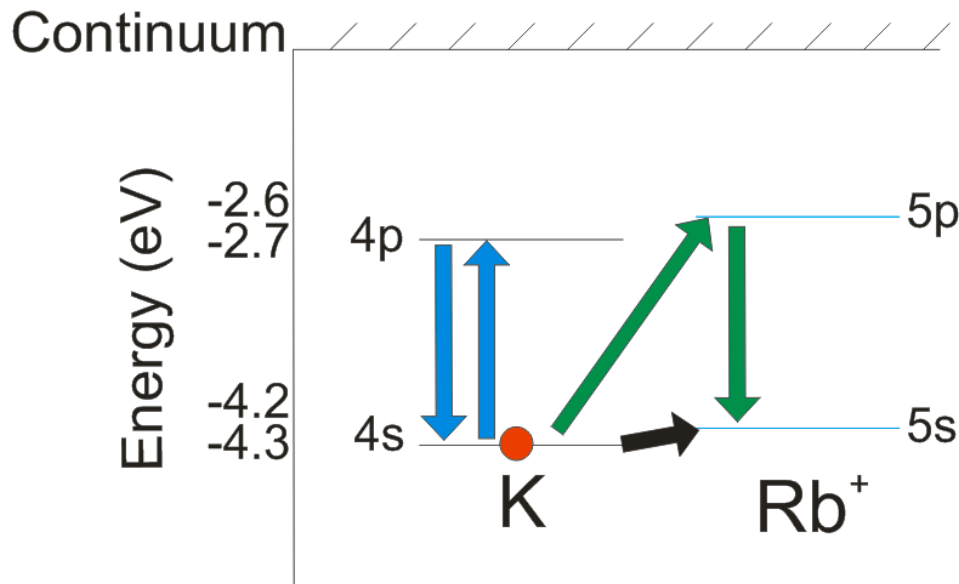


Mainz/ISOLDE

# Rb<sup>+</sup> on K Charge Exchange

CEC tested at the University of Mainz  
TRIGA-Laser facility in July 2010

Charge exchange between Rb<sup>+</sup> and K  
is nearly resonant



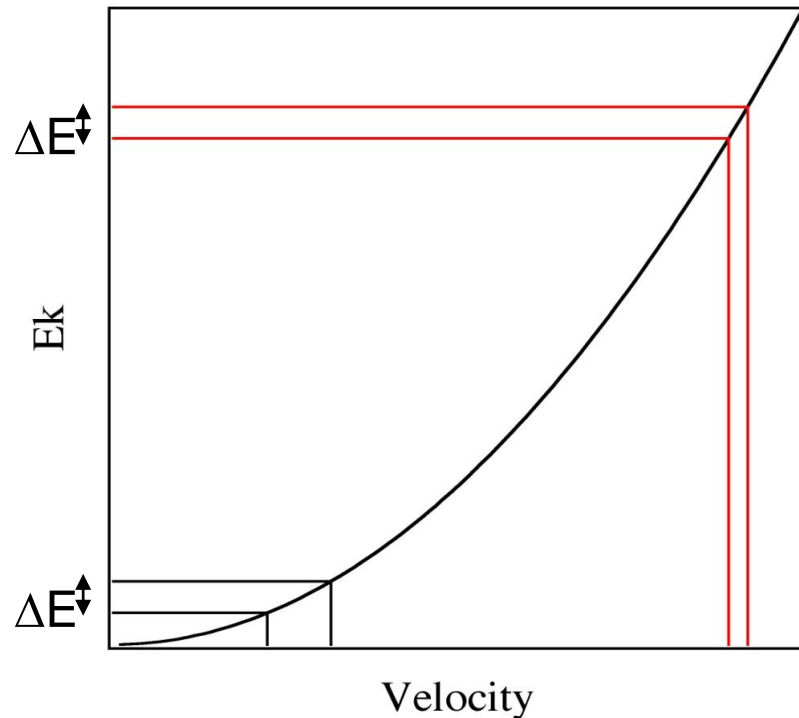
- The fraction of Rb that is neutralized depends on:
  - Cross section ( $\sigma$ )
  - K vapor density ( $n$ )
  - Interaction length ( $l$ )

$$\text{Neutral fraction} = 1 - e^{-n\sigma l}$$

# Velocity Bunching

Doppler broadening increases the linewidth of the excitation from the natural linewidth, which is problematic

By accelerating the ion beam velocity bunching occurs which allows for a decrease in Doppler broadening.



For a given  $\Delta E \rightarrow$

smaller  $\Delta v$

at high kinetic energy ( $E_k$ )  $\rightarrow$

reduced Doppler broadening

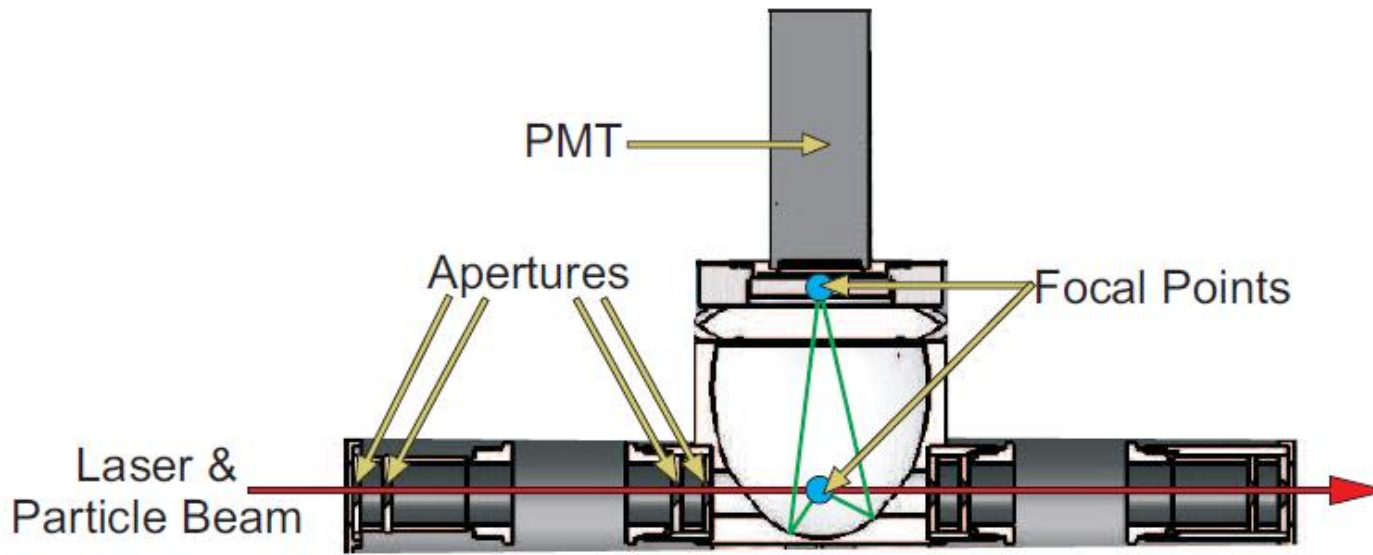
# Bias Voltage to CEC

## Requirements:

- feasibility to scan voltage  $\pm 10$  kV
  - »  $\pm 110$  GHz for 60 keV Ca II
- stability better than  $10^{-5}$ 
  - » 0.6 V for 60 kV acceleration voltage;  $\sim 7$  MHz linewidth
- switching speed less than 1 ms
  - » fast scan around resonance to reduce systematic error from system fluctuations
- recovery time less than a few hundreds ms
  - » no data taking during transition -> less efficient
- measure acceleration voltage
  - » voltage divider: requires  $10^{-5}$  precision in dividing R
- frequent reference isotope measurement
  - » each measurement sandwiched by reference measurements
  - » feasibility to quickly go back and forth between two isotopes
  - » each measurement less than 1 hour and requires high counting rate
- collinear/anticollinear spectroscopy

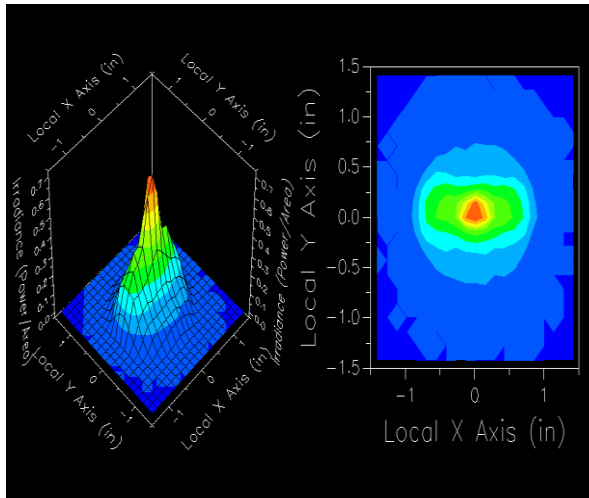


# NSCL Photon Detection System

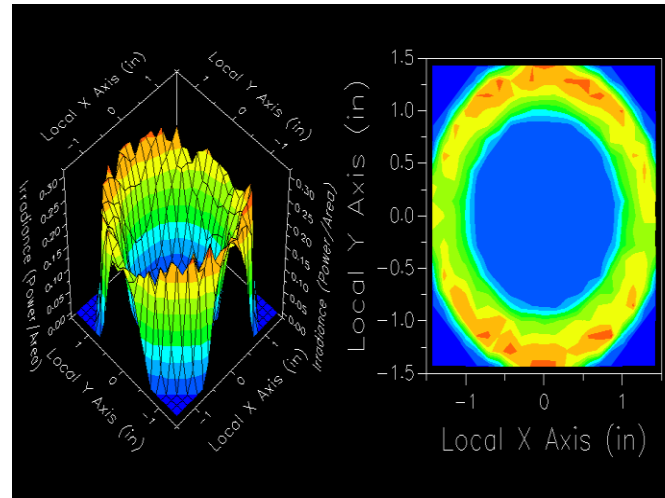


- Elliptical reflector to collect photons
- Apertures along light path to reduce scattered light
- Collimator at face of PMT to block stray light from reflector

Signal collection

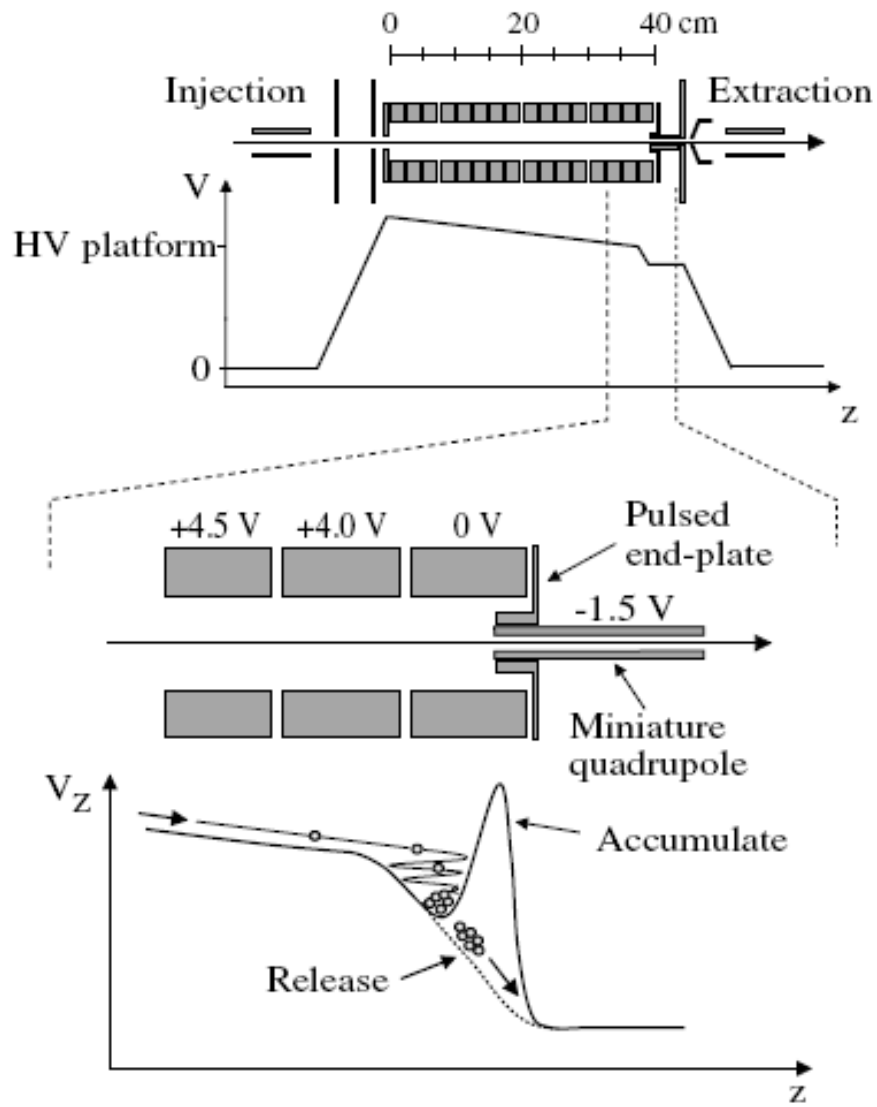


Scattered light



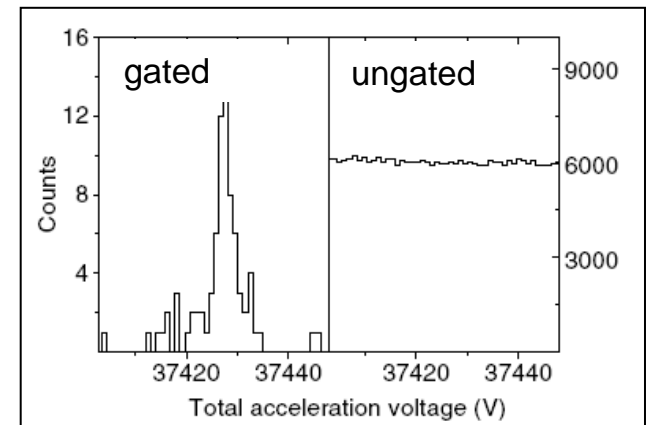
Simulations performed with FRED optical engineering software

# Cooler Buncher at IGISOL



Ion guide + fusion reaction provided access to neutron-deficient, refractive lanthanides for laser spectroscopy measurements

$^{174}\text{Hf}$  (stable)



$1300 \text{ s}^{-1}$  25 min collection

Bunch width  $< 20 \mu\text{s}$   
 Energy spread  $< 10^{-5}$  of 40 keV  
 Emittance  $3\pi\text{-mm-mrad}$

# Laser Spectroscopy Summary

- Deduce the size and shape the nucleus
  - Isotope shifts
  - Charge radii
  - Nuclear moments ( $\mu$ ,  $Q$ )
- Applicable over a wide range of  $T_{1/2}$  values, hence measurements made across long isotopic chains
- Several methods for measuring hyperfine spectra
- Increased sensitivity by
  - Improving photon counting geometry
  - Using bunched beams
  - Tailoring detection methods to specific elemental properties
- Explore new laser excitation schemes
  - Access to unstudied elements

